IEEE Access
Multidisciplinary | Rapid Review | Open Access Journal

SPECIAL SECTION ON SOCIETY SECTION: IEEE BROADCAST TECHNOLOGY SOCIETY SECTION

Received February 17, 2020, accepted March 12, 2020, date of publication March 18, 2020, date of current version March 31, 2020.

*Digital Object Identifier 10.1109/ACCESS.2020.2981638*

# Probabilistic Analysis on Successive Cancellation-Assisted Transmitter Identification in SFN With Randomly Distributed Co-Channel Interferers

**SUNGJUN AHN, (Member, IEEE), SUNG-IK PARK, (Senior Member, IEEE), SUNHYOUNG KWON, (Member, IEEE), JAE-YOUNG LEE, (Senior Member, IEEE), AND NAMHO HUR, (Member, IEEE)**

Media Research Division, Electronics and Telecommunications Research Institute (ETRI), Daejeon 305-700, South Korea

Corresponding author: Sungjun Ahn (sjahn@etri.re.kr)

This work was supported by the Institute for Information and Communications Technology Planning and Evaluation (IITP) Grant funded by the Korean Government (MSIT) (Development of Transmission Technology for Ultra High Quality UHD) under Grant 2017-0-00081.

**ABSTRACT** This paper investigates the detection error of radio frequency (RF)-watermark type transmitter identification (TxID) signal in a single frequency network (SFN). Based on the Cramer-Rao bound (CRB) of TxID detection, closed-form failure probabilities for TxID detection are derived. In order to reflect the practical network condition, the interference from Poisson-distributed out-of-guard interval transmitters is accounted for TxID detection failure probability (TDFP). The proposed approach consequently examines the possible TDFP gain that can be obtained by applying successive preamble cancellation to the TxID detection. Numerical results reveal that the performance of the preamble cancellation-assisted technique is dependent on the threshold signal-to-interference noise ratio (SINR) for preamble signal detection. Nevertheless, the assistance of preamble cancellation is verified to guarantee more than 4 dB improvement of TxID detection capability under practical preamble signal configurations.

**INDEX TERMS** Transmitter identification (TxID), successive interference cancellation (SIC), Poisson point process (PPP).

## I. INTRODUCTION

The modern broadcast systems are likely to be deployed single frequency network (SFN)-based, due to a lack of spectrum resources [1]–[5]. However, SFNs have a potential inter-symbol interference problem since the broadcast signals lagged more than an acceptable delay range (i.e., guard interval or time-domain window size) rather bother the signal decoding [6]. Moreover, the SFN may produce some additional multipath, so that degrade the reception quality. For a neat SFN operation, the network should be organized appropriately through careful determinations of the transmitter (Tx) site, emission times, guard interval, etc [7].

For efficient construction and management of SFN, a concept so-called transmitter identification (TxID) has been introduced in [8]. The proposed TxID is enabled by a certain set of separable signals (namely, TxID signals), so that allows the receiver (Rx) to extract the contribution of each co-existing Tx to the net receive channel gain when each Tx transmits different TxID signal at the same time. This approach lies in the radio frequency (RF) layer based on spread spectrum transmissions [9], [10], unlike a signaling field insertion in the transport layer [11], [12]. Hence, such type of TxID technologies has been called as an RF-watermark or a fingerprint technique. In the commercial, the RF-watermark type TxID has been adopted in Advanced Television System Committee (ATSC) 1.0 and 3.0 standards [13]–[16]. In the ATSC protocols, TxID sequences are generated in a pseudo-random noise (PN) manner and superposed with preamble signals (if TxID is intended). The Rx can therefore acquire the per-Tx channel components by taking a correlation between a known TxID sequence (of interest) and the received signal.

Beyond the intended role itself, the supplementary applications of the RF-watermark TxID signal have gathered the broadcasters' interest as well [15]. One convincing use case is an advanced channel estimation. As TxID detections inform about time-domain channel signatures, it is

The associate editor coordinating the review of this manuscript and approving it for publication was Wei Li.

able to improve a channel estimation accuracy by using the multipath-awareness.[1] For example, a windowing-based method in [17], [18] and a subspace projection-based approach extending the idea of [19] are possible. On the other hand, the use cases in other verticals have been noted as well. Specifically, encouraging proposals for wireless positioning and additive data transmission have been reported in previous literature [20]–[23]. Relying on the robustness and resiliency of terrestrial digital television (DTV) infrastructure against macro-scale disasters, those applied solutions are expected promising especially for ensuring public safety in emergency situations [15], [24], [25].

In effect, the RF-watermark type TxID is inherently interfered by preamble signals since the TxID signal is buried under the preambles. Although the TxID sequences are designed to have good auto- and cross-correlation properties enough to tolerate the preamble interference, there still exists a considerable degradation[2] [15], [26]. Therefore, [1] has introduced an advanced TxID detection technique that cancels preambles from the received signal in advance. As well, various simulations, laboratory tests, and field trials in [1] have verified the improvement of TxID signal quality from preamble cancellation to be substantial. However, the performance of the TxID detection (including not only a performance of the preamble cancellation-assisted scheme but also that of the conventional scheme) in terms of how frequent the detection failure is, has yet been verified so far.

In this paper, a theoretic analysis is addressed on the error performance of the preamble cancellation-assisted TxID detection (PCTD). The TxID detection failure probability (TDFP) of the PCTD is derived using the Cramer-Rao bound (CRB), a well-known and tight lower bound of estimation error variance, as an indicator for detection accuracy [27]. The analysis is conducted in a stochastic geometry framework reflecting the existence of the out-of-guard interval Txs, which are regarded as co-channel interferers.[3] In order to provide practical insight, the problem is further carefully tackled by explicitly embodying the SIC error propagation effect in the system model. Based on the analytic derivations given in closed-forms, the theoretic gain of preamble cancellation is verified through various comparisons against the conventional TxID detection method.

The rest of the paper is organized as follows. In Section II, the considered TxID detection system in SFN is described. Based on the system model, TDFPs of the conventional detection and the PCTD are obtained in Section III and Section IV, respectively. Numerical results with corresponding discussions are presented in Section VI, and Section VII concludes the paper with some remarks.

[1]Following the regular use in the broadcast industry, the term *TxID detection* in this paper generically includes a channel signature (time-delay) estimation, not limited to the strict detection of TxID code (sequence).

[2]An ensemble averaging over some frames enhances the detection performance, but the averaging cannot overcome a fundamental degradation from the preamble interference.

[3]This work was partially presented at IEEE BMSB [28].

*Notation* : $\Pr[\mathbb{A}]$ indicates a probability of an event $\mathbb{A}$; $\Pr[\mathbb{A}|\mathbb{B}]$ indicates a probability of an event $\mathbb{A}$ conditioned to an event $\mathbb{B}$; $\mathbb{E}_X[\cdot]$ denotes an expectation over a random variable $X$; $\exp(\cdot)$ stands for the exponential function $e^{(\cdot)}$; $|\mathcal{A}|$ denotes the cardinality of a set $\mathcal{A}$; $\Gamma(z)=\int_0^\infty x^{z-1}\exp(-x)dx$ for $\Re\mathfrak{e}(z)>0$ denotes the Gamma function.

## II. SYSTEM MODEL

For the baseline system model, an SFN that consists of multiple Txs is considered. In this model, the universal set of the Tx can be partitioned into two distinct subsets, $\Phi_{\mathrm{T}}$ and $\Phi_{\mathrm{T}}^c$: $\Phi_{\mathrm{T}}$ is the group of Txs which contributes to the quality of the after-equalization signal, while $\Phi_{\mathrm{T}}^c$ is the set of the out-of-guard interval Txs. The Txs in $\Phi_{\mathrm{T}}^c$ are assumed to be geometrically distributed by homogeneous Poisson point process (PPP) with intensity $\kappa$, particularly in the area distanced more than $r_0$ from the Rx. Each Tx is assumed to inject its own TxID sequence into the transmit host signals (preamble signals, when we follow the ATSC systems) with an injection level $\delta<1$ i.e., the Txs allocate $\delta$ times of host signal power $P_{\mathrm{T}}$: $\delta P_{\mathrm{T}}$ for TxID transmission. Then the received signal at the Rx can be modeled as

$$Y[t]=\sum_{i\in\Phi_{\mathrm{T}}}\frac{H_i}{d_i^{\alpha/2}}(X_i[t]+Z_{\mathrm{p},i}[t])+\sum_{k\in\Phi_{\mathrm{T}}^c}\frac{H_k}{d_k^{\alpha/2}}(X_k[t]+Z_{\mathrm{p},k}[t])+W[t], \quad (1)$$

where $H_i$, $X_i[t]$ and $Z_{\mathrm{p},i}[t]$ for $i\in\Phi_{\mathrm{T}}\cup\Phi_{\mathrm{T}}^c$ denote the channel gain, TxID signal, and host signal from the $i$th Tx, which correspond to the reception at time $t\geq 0$. $W[t]$ denotes an additive white Gaussian noise (AWGN), and each $H_i$s, $X_i[t]$s, $Z_{\mathrm{p},i}[t]$s, and $W[t]$ is assumed as a zero-mean complex Gaussian r.v. with unit variance. In addition, having the property of the TxID sequences defined in [13] and [14], the TxID sequences are assumed to be relatively uncorrelated. Meantime, a large-scale channel fading based on the standard path-loss model with exponent $\alpha$ is considered, where $d_i$s for $i\in\Phi_{\mathrm{T}}\cup\Phi_{\mathrm{T}}^c$ are the distances of Tx-to-Rx path.

Moivated by [16], a signal-to-DTV noise ratio (SDR) of the $i\in\Phi_{\mathrm{T}}$th Tx's TxID signal at the Rx is given by

$$\gamma_i=\frac{\frac{|H_i|^2\delta P_{\mathrm{T}}}{d_i^\alpha}}{1+\zeta P_{\mathrm{T}}+\frac{|H_i|^2P_{\mathrm{T}}}{d_i^\alpha}+\sum_{j\in\Phi_{\mathrm{T}}\setminus i}\frac{|H_j|^2P_{\mathrm{T}}}{d_j^\alpha}}, \quad (2)$$

where the undesired signals from outside of the guard distance $r_0$ are treated as random noise. $\zeta P_{\mathrm{T}}$ stands for the corresponding interference term, where the aggregate channel gain across the co-channel interferers is defined as $\zeta\triangleq\sum_{k\in\Phi_{\mathrm{T}}^c}\frac{|H_k|^2}{d_k^\alpha}$.

## III. CRB AND TDFP IN RANDOM INTERFERER NETWORKS: CONVENTIONAL TxID DETECTION CASE

In this section, a CRB and a TDFP in SFN with multiple Txs ($T\triangleq|\Phi_{\mathrm{T}}|$ in particular) is derived. The case without

using preamble cancellation, which will be hereafter referred to as *conventional TxID detection (CTD)*, is first addressed in this section before turning into PCTD in Section IV. Inspired from [29], a CRB of the conventional TxID detection based on cross-correlation method can be obtained as

$$\sigma_{i,\tau}^2 = \frac{3}{\pi^2 M \gamma_i} = \frac{1+\zeta P_{\mathrm{T}} + \frac{|H_i|^2 P_{\mathrm{T}}}{d_i^\alpha} + \sum_{j\in\Phi_{\mathrm{T}}\setminus i} \frac{|H_j|^2 P_{\mathrm{T}}}{d_j^\alpha}}{\frac{\pi^2 M}{3}\cdot\frac{|H_i|^2\delta P_{\mathrm{T}}}{d_i^\alpha}}, \tag{3}$$

where the problem of TxID detection in [16] is identical to obtaining a time delay of $Y[t]$ from the given noise-free TxID sequence. To be noted, $M$ denotes the length of TxID sequences.

*Proposition 1*: *For the CTD case, TDFP-namely the $\epsilon$-outage probability-for detecting the ith Tx's TxID signal conditioned to $\Phi_T$ and $\Phi_T^c$, which is defined as*

$$\Pr[\sigma_{i,\tau}^2 \geq \epsilon | \Phi_{\mathrm{T}}, \Phi_{\mathrm{T}}^c] = Pr\left[\frac{(\epsilon\pi^2 M\delta - 3)P_{\mathrm{T}}}{d_i^\alpha}|H_i|^2 - 3\sum_{j\in\Phi_{\mathrm{T}}\setminus i}\frac{|H_j|^2 P_{\mathrm{T}}}{d_j^\alpha} \leq 3(\zeta P_{\mathrm{T}}+1)\right], \tag{5}$$

*is given as (4), shown at the bottom of this page, for $\forall\epsilon > 0$.*[4]

*Proof:* Without loss of generality, let $i = 1$. Let the random variable $(\epsilon\pi^2 M\delta - 3)d_1^{-\alpha}P_{\mathrm{T}}|H_1|^2$ be $\nu_1$ and denote $3P_{\mathrm{T}}d_k^{-\alpha}|H_k|^2$s as $\nu_k$ for $k$=2,$\cdots$, $T$. It can be easily noticed that $\nu_1,\cdots,\nu_T$ are exponentially distributed, where the distribution parameters $\lambda_1,\cdots,\lambda_T$ for each of $\nu_k$s are given $d_1^\alpha/(\epsilon\pi^2 M\delta-3)/P_{\mathrm{T}}, d_2^\alpha/3/P_{\mathrm{T}},\cdots, d_T^\alpha/3/P_{\mathrm{T}}$, respectively.

Since the moment generating function (MGF) for the probability density function (pdf) of an exponential distribution with rate parameter $\chi$ is given $\mathcal{M}_{f_\chi}(s) = \chi/(js+\chi)$, the MGF for $\nu_1 - \sum_{k=2}^T \nu_k$ is found

$$\mathcal{M}_{f_{\boldsymbol{\lambda}}}(s) = \frac{\prod_{k=1}^T \lambda_k}{(js+\lambda_1)\prod_{l=2}^T(-js+\lambda_l)}. \tag{6}$$

Besides, (6) can be expanded in a form of weighted summation among $(js+\lambda_1)^{-1}$ and $(-js+\lambda_2)^{-1},\cdots,(js+\lambda_T)^{-1}$. An appropriate arrangement over the summation components returns

$$\mathcal{M}_{f_{\boldsymbol{\lambda}}}(s) = \left(\frac{1}{\lambda_1}\right)^{T-2}\frac{1}{\prod_{k=2}^T\left(\frac{1}{\lambda_1}+\frac{1}{\lambda_k}\right)}\cdot\frac{1}{js+\lambda_1} - \sum_{k=2}^T\left(\frac{1}{\lambda_k}\right)^{T-2}\frac{1}{\left(\frac{1}{\lambda_1}+\frac{1}{\lambda_k}\right)\prod_{\substack{2\leq l\leq T\\ l\neq k}}\left(\frac{1}{\lambda_k}-\frac{1}{\lambda_l}\right)}\cdot\frac{1}{-js+\lambda_k}, \tag{7}$$

[5]which gives the expression of pdf $f_{\boldsymbol{\lambda}}(x)$ in the form of

$$f_{\boldsymbol{\lambda}}(x) = \left(\frac{1}{\lambda_1}\right)^{T-2}\frac{1}{\prod_{k=2}^T\left(\frac{1}{\lambda_1}+\frac{1}{\lambda_k}\right)}e^{-\lambda_1 x}u(x) - \sum_{k=2}^T\left(\frac{1}{\lambda_k}\right)^{T-2}\frac{1}{\left(\frac{1}{\lambda_1}+\frac{1}{\lambda_k}\right)\prod_{\substack{2\leq l\leq T\\ l\neq k}}\left(\frac{1}{\lambda_k}-\frac{1}{\lambda_l}\right)}e^{\lambda_k x}u(-x) \tag{8}$$

where $u(\cdot)$ denotes a unit step function. The integration over (8) consequently yields (4), as shown at the bottom of this page, since $3(\zeta P_{\mathrm{T}}+1) > 0$ holds. ■

Subsequently, without an exact knowledge of $\Phi_{\mathrm{T}}^c$, the expected TDFP can be calculated by averaging $\Pr[\sigma_{i,\tau}^2 \geq \epsilon|\Phi_{\mathrm{T}},\Phi_{\mathrm{T}}^c]$ over all possible sets of $\Phi_{\mathrm{T}}^c$. During the Txs of $\Phi_{\mathrm{T}}^c$ are distributed with homogeneous PPP, the closed-form expression of $\Pr[\sigma_{i,\tau}^2 \geq \epsilon|\Phi_{\mathrm{T}}]$ can be obtained by following theorem.

*Theorem 1: The TDFP of CTD with expectation over all possible sets of $\Phi_T^c$ is expressed as (9), shown at the bottom of the next page, for a given set of $\Phi_T$.*

*Proof:* Based on Proposition 1, (9) is achieved where (a) holds since the MGF of $\zeta$ is given by $\mathbb{E}_{\Phi_{\mathrm{T}}^c}[\exp(-s\zeta)] = \exp\{-\pi\kappa(s^{2/\alpha}\Gamma(1-2/\alpha)\Gamma(1+2/\alpha) - r_0^2(1-2r_0^\alpha/(s(\alpha+2))_2F_1(1,1+2/\alpha;2+2/\alpha;-r_0^\alpha/s))\} \triangleq \mathcal{M}_\zeta(s)$[6] where ${}_2F_1(a,b;c;t)$ is a Gauss hypergeometric function. ■

*Remark (Monotonic Decrease of TDFP Over $\delta$):* As can be intuitively inferred, TDFP of CTD monotonically decreases by $\delta$. Note that the event space in (5), the space of tuples $(H_1,\cdots H_T)$ that satisfy $\sigma_{i,\tau}^2 \geq \epsilon$ in other words, shrinks when $\delta$ gets increased. It is straightforward that increasing

[4]The TDFP defined in this paper can be considered as an eligible measure for the TxID detection performance [27]. The integration of TDFP over possible $\epsilon$s gives the expected CRB, i.e., $\int_0^\infty \Pr[\sigma_{i,\tau}^2 \geq \epsilon|\Phi_{\mathrm{T}}]d\epsilon = \mathbb{E}_{\Phi_{\mathrm{T}}^c,\{H_i\}_{i\in\Phi_{\mathrm{T}}}}[\sigma_{i,\tau}^2|\Phi_{\mathrm{T}}]$ [30]. The probabilistic approach is especially meaningful for addressing PCTD, since it enables accounting the effect of preamble cancellation failures.

[5]A substitution method can simply show the equivalence between (6) and (7).

[6]For detailed derivation, see [31], [32], and therein.

$$\Pr[\sigma_{i,\tau}^2 \geq \epsilon|\Phi_{\mathrm{T}},\Phi_{\mathrm{T}}^c] = 1 - \left(\frac{\epsilon\pi^2 M\delta - 3}{d_i^\alpha}P_{\mathrm{T}}\right)^{T-1}\prod_{\substack{1\leq j\leq T\\ j\neq 1,i}}\frac{1}{\left(\frac{\epsilon\pi^2 M\delta-3}{d_i^\alpha}+\frac{3}{d_j^\alpha}\right)P_{\mathrm{T}}}\exp\left(-\frac{d_i^\alpha 3(\zeta P_{\mathrm{T}}+1)}{(\epsilon\pi^2 M\delta-3)P_{\mathrm{T}}}\right)$$

$$\Pr[\sigma_{i,\tau}^2 \geq \epsilon|\Phi_{\mathrm{T}}] = \mathbb{E}_{\Phi_{\mathrm{T}}^c}\left[\Pr[\sigma_{i,\tau}^2 \geq \epsilon|\Phi_{\mathrm{T}},\Phi_{\mathrm{T}}^c]\right] \tag{4}$$

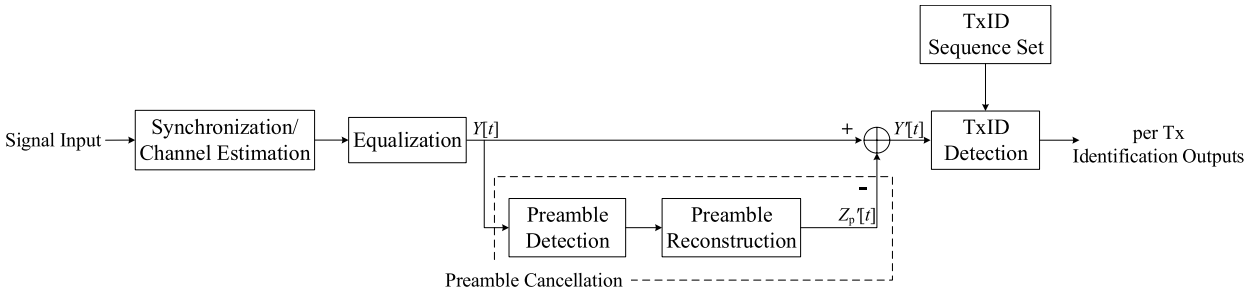


**FIGURE 1.** Block diagram of PCTD procedure.

the power of TxID signals improves the desired SDR, consequently decreasing TDFP.

Following Theorem 1, dealing with uniformly distributed $T$ Txs in the Rx-centered disk with radius $r_0$, the following corollary is obtained:

*Corollary 1*: *With a uniform distribution of Txs in* $\Phi_T$, *the average TDFP of CTD accounting of all the possible sets of* $\Phi_T$ *and* $\Phi_T^c$ *is given by*

$$\begin{aligned}&\Pr[\sigma_{i,\tau}^2 \geq \epsilon] \\ &= \mathbb{E}_{\Phi_\mathrm{T}}[\Pr[\sigma_{i,\tau}^2 \geq \epsilon | \Phi_\mathrm{T}]] \\ &= 1 - \int_0^{r_0} \cdots \int_0^{r_0} \left(\frac{2T}{r_0^2}\right)^T r_1 \cdots r_T \Pr[\sigma_{i,\tau}^2 \geq \epsilon | \Phi_\mathrm{T}] dr_T \cdots dr_1\end{aligned} \tag{10}$$

while a tractable closed-form solution is not straightforward.

## IV. TDFP OF PCTD

Since preamble signals have to be decoded at the Rxs, the Rx with a TxID functional can effectively enhance the TxID signal quality by canceling preamble from the received signal. Pointing out the opportunity to enhance the TxID signal quality, [1] has proposed several schemes for PCTD. Based on the concept proposed in [1], this section analyzes the TDFP performance of the PCTD in stochastic perspective. We here emphasize that the error propagation effect is explicitly considered in the SIC model, which fine-tunes the analyses to be feasible in practice.

### A. PCTD PROCESS

The block diagram in FIGURE 1 illustrates the process of PCTD. With preamble cancellation applied, the effective received signal can be written by

$$\begin{aligned}Y[t] = &\sum_{i \in \Phi_\mathrm{T}} \frac{H_i}{d_i^{\alpha/2}} (X_i[t] + Z_\mathrm{p}[t] - \hat{Z}_\mathrm{p}[t]) \\ &+ \sum_{k \in \Phi_\mathrm{T}^c} \frac{H_k}{d_k^{\alpha/2}} (X_k[t] + Z_{\mathrm{p},k}[t]) + W[t],\end{aligned} \tag{11}$$

where the estimated preamble symbol is given by a conditional form $\hat{Z}_\mathrm{p}[t] = Z_\mathrm{p}[t]\mathbf{1}(\mathcal{C}) + Z'\mathbf{1}(\mathcal{E})$, which is subjected to the success and failure of preamble detection, having a realization of SIC error propagation $Z'$ as a complex Gaussian random variable with zero mean and unit variance.

### B. TDFP ANALYSIS

Having the host preamble signal canceled successfully, the Rx can increase the SDRs of TxID signals from (2) substantially. However, it should be noticed that preamble detection can also be failed, and the TxID SDR can rather decrease in this case. The TDFP is therefore given by a summation of two joint probabilities which are subjected to the success/failure of preamble detection, as $\Pr[\sigma_{i,\tau}^2 \geq \epsilon | \Phi_\mathrm{T}, \gamma_\mathrm{th}] = \Pr[\sigma_{i,\tau}^2(\mathcal{C}) \geq \epsilon, \gamma_\mathrm{p} \geq \gamma_\mathrm{th} | \Phi_\mathrm{T}] + \Pr[\sigma_{i,\tau}^2(\mathcal{E}) \geq \epsilon, \gamma_\mathrm{p} < \gamma_\mathrm{th} | \Phi_\mathrm{T}]$. The conditioned variables here,

$$\sigma_{i,\tau}^2(\mathcal{C}) = \frac{1 + \zeta P_\mathrm{T}}{\frac{\pi^2 M}{3} \cdot \frac{|H_i|^2 \delta P_\mathrm{T}}{d_i^\alpha}} \tag{12}$$

and

$$\sigma_{i,\tau}^2(\mathcal{E}) = \frac{1 + \zeta P_\mathrm{T} + \frac{2|H_i|^2 P_\mathrm{T}}{d_i^\alpha} + \sum_{j \in \Phi_\mathrm{T} \setminus i} \frac{2|H_j|^2 P_\mathrm{T}}{d_j^\alpha}}{\frac{\pi^2 M}{3} \cdot \frac{|H_i|^2 \delta P_\mathrm{T}}{d_i^\alpha}}, \tag{13}$$

imply the CRBs for detecting the $i$th Tx's TxID signal under success and failure of preamble detection, respectively.

$$\begin{aligned}&\overset{(a)}{=} 1 - \left(\frac{\epsilon \pi^2 M \delta - 3}{d_i^\alpha} P_\mathrm{T}\right)^{T-1} \exp\left(-\frac{3 d_i^\alpha}{(\epsilon \pi^2 M \delta - 3) P_\mathrm{T}}\right) \prod_{\substack{1 \leq j \leq T \\ j \neq 1, i}} \frac{1}{\left(\frac{\epsilon \pi^2 M \delta - 3}{d_i^\alpha} + \frac{3}{d_j^\alpha}\right) P_\mathrm{T}} \exp\left\{-\pi \kappa \left(\left(\frac{3 d_i^\alpha}{\epsilon \pi^2 M \delta - 3}\right)^{2/\alpha} \Gamma\left(1 + \frac{2}{\alpha}\right) \Gamma\left(1 - \frac{2}{\alpha}\right) - r_0^2 \left(1 \right.\right.\right. \\ &\left.\left.\left. - \frac{2 r_0^\alpha (\epsilon \pi^2 M \delta - 3)}{3 d_i^\alpha (\alpha + 2)} {}_2F_1\left(1, 1 + \frac{2}{\alpha}; 2 + \frac{2}{\alpha}; -r_0^\alpha \frac{\epsilon \pi^2 M \delta - 3}{3 d_i^\alpha}\right)\right)\right\}\end{aligned} \tag{9}$$

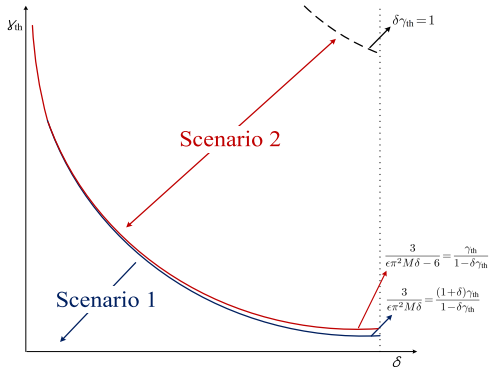


**FIGURE 2.** Feasible ($\delta$, $\gamma_{\text{th}}$) regions for PCTD scenarios.

In addition, $\gamma_{\text{th}}$ denotes the threshold signal-to-interference plus noise ratio (SINR) of preamble detection, threshold of cancellation (ToC) in other words, where the SINR of preamble signal is expressed as

$$\gamma_{\text{p}} = \frac{\sum_{l\in\Phi_{\text{T}}} \frac{|H_l|^2 P_{\text{T}}}{d_l^{\alpha}}}{1+\sum_{l\in\Phi_{\text{T}}} \frac{\delta|H_l|^2 P_{\text{T}}}{d_l^{\alpha}} + \zeta(1+\delta)P_{\text{T}}}. \tag{14}$$

The conditional probabilities $\Pr[\sigma^2_{i,\tau}(\mathcal{C}) \geq \epsilon, \gamma_{\text{p}} < \gamma_{\text{th}}|\Phi_{\text{T}}]$ and $\Pr[\sigma^2_{i,\tau}(\mathcal{E}) \geq \epsilon, \gamma_{\text{p}} \geq \gamma_{\text{th}}|\Phi_{\text{T}}]$ are obtained by Theorem 2 and 3 below, respectively. To be noticed, the preamble signals can be configured more robust than TxID at detection, while vice versa is also available. The expressions (12) - (14) yield that the channel gain thresholds for preamble and TxID detection are $\frac{3}{\epsilon\pi^2 M\delta}$ or $\frac{3}{\epsilon\pi^2 M\delta-6}$ and $\frac{\gamma_{\text{th}}}{1-\delta\gamma_{\text{th}}}$, respectively when co-channel interference does not exist. Our approach tackles the cases $\frac{3}{\epsilon\pi^2 M\delta} \geq \frac{(1+\delta)\gamma_{\text{th}}}{1-\delta\gamma_{\text{th}}}$ and $\frac{3}{\epsilon\pi^2 M\delta-6} < \frac{\gamma_{\text{th}}}{1-\delta\gamma_{\text{th}}}$,[7] i.e., the case preamble more robust than TxID and the case TxID more robust than preamble, separately. The regions of $\delta$ and $\gamma_{\text{th}}$ that correspond to each scenario are schematically depicted in FIGURE 2. Since the curves $\frac{3}{\epsilon\pi^2 M\delta} = \frac{(1+\delta)\gamma_{\text{th}}}{1-\delta\gamma_{\text{th}}}$ and $\frac{3}{\epsilon\pi^2 M\delta-6} = \frac{\gamma_{\text{th}}}{1-\delta\gamma_{\text{th}}}$ differ slightly, the intractable cases lie in very limited region, so that makes our approach feasible.

### 1) SCENARIO 1 ($\mathcal{S}_1$): PREAMBLE MORE ROBUST THAN TxID SIGNAL ($\frac{3}{\epsilon\pi^2 M\delta} \geq \frac{(1+\delta)\gamma_{\text{th}}}{1-\delta\gamma_{\text{th}}}$)

Since the signal measurement and channel analysis are usually obtained at the sites preamble can be detected, the network operator may use the signal parameters which allows the preamble be more robust than TxID signals. Such signal parameters let the TxID detector suffer less from additional noise due to a mis-cancellation $-\hat{Z}_{\text{p}}[t] = -Z'$ in (11). In this subsection, we show that the condition $\frac{3}{\epsilon\pi^2 M\delta} \geq \frac{(1+\delta)\gamma_{\text{th}}}{1-\delta\gamma_{\text{th}}}$ allows more tuples of $(H_1, \cdots H_{|\Phi_{\text{T}}|})$ to decrease the TDFP by preamble cancellation, compared to $\frac{3}{\epsilon\pi^2 M\delta-6} < \frac{\gamma_{\text{th}}}{1-\delta\gamma_{\text{th}}}$ case. The TDFP at the TxID detector utilzing preamble cancellation is derived by Theorem 2 and 3 as follows.

*Theorem 2*: *Within Scenario 1, the joint probability of TxID failure and preamble detection success is given by*

$$\begin{aligned}
&\Pr[\sigma^2_{i,\tau}(\mathcal{C}) \geq \epsilon, \gamma_{\text{p}} \geq \gamma_{\text{th}}|\Phi_{\text{T}}, \mathcal{S}_1] \\
&= \sum_{j\in\Phi_{\text{T}}\setminus i} \exp\left(-\frac{d_i^{\alpha}\gamma_{\text{th}}}{P_{\text{T}}(1-\delta\gamma_{\text{th}})}\right) \frac{\mathcal{M}_{\zeta}\left(\frac{d_i^{\alpha}(1+\delta)\gamma_{\text{th}}}{1-\delta\gamma_{\text{th}}}\right)}{(\frac{d_i^{\alpha}}{d_j^{\alpha}}-1)\prod_{k\in\Phi_{\text{T}}\setminus\{i,j\}}\left(1-\frac{d_j^{\alpha}}{d_k^{\alpha}}\right)} \\
&\quad + \sum_{j\in\Phi_{\text{T}}\setminus i} \exp\left(-\frac{d_j^{\alpha}\gamma_{\text{th}}}{P_{\text{T}}(1-\delta\gamma_{\text{th}})}\right) \frac{\left(\frac{d_i^{\alpha}}{d_j^{\alpha}}-2\right)\mathcal{M}_{\zeta}\left(\frac{d_j^{\alpha}(1+\delta)\gamma_{\text{th}}}{1-\delta\gamma_{\text{th}}}\right)}{\left(\frac{d_i^{\alpha}}{d_j^{\alpha}}-1\right)\prod_{k\in\Phi_{\text{T}}\setminus\{i,j\}}\left(1-\frac{d_j^{\alpha}}{d_k^{\alpha}}\right)} \\
&\quad - \exp\left(-\frac{3d_i^{\alpha}}{P_{\text{T}}\epsilon\pi^2 M\delta}\right)\mathcal{M}_{\zeta}\left(-\frac{3d_i^{\alpha}}{\epsilon\pi^2 M\delta}\right)
\end{aligned} \tag{15}$$

*for a given set of* $\Phi_T$.

*Proof:* From the definition, we obtain the followings:

$$\begin{aligned}
&\Pr[\sigma^2_{i,\tau}(\mathcal{C}) \geq \epsilon, \gamma_{\text{p}} \geq \gamma_{\text{th}}|\Phi_{\text{T}}, \Phi^c_{\text{T}}, \mathcal{S}_1] \\
&= \Pr\left[-\sum_{j\in\Phi_{\text{T}}\setminus i}\frac{P_{\text{T}}}{d_j^{\alpha}}|H_j|^2 + \frac{\gamma_{\text{th}}(1+(1+\delta)\zeta P_{\text{T}})}{1-\delta\gamma_{\text{th}}} \leq \frac{P_{\text{T}}}{d_i^{\alpha}}|H_i|^2 \right. \\
&\quad \left. \leq \frac{3(1+\zeta P_{\text{T}})}{\epsilon\pi^2 M\delta}\right] \\
&\overset{(a)}{=} \int_0^{c(\zeta)} \left\{\exp\left(-\frac{d_i^{\alpha}}{P_{\text{T}}}\left(y - \frac{\gamma_{\text{th}}(1+(1+\delta)\zeta P_{\text{T}})}{1-\delta\gamma_{\text{th}}}\right)\right)\right. \\
&\quad \left. - \exp\left(-\frac{3d_i^{\alpha}(1+\zeta P_{\text{T}})}{P_{\text{T}}\epsilon\pi^2 M\delta}\right)\right\} \sum_{j\in\Phi_{\text{T}}\setminus i} \frac{\exp(-\frac{d_j^{\alpha}y}{P_{\text{T}}})}{\frac{P_{\text{T}}}{d_j^{\alpha}}\prod_{k\in\Phi_{\text{T}}\setminus\{i,j\}}\left(1-\frac{d_j^{\alpha}}{d_k^{\alpha}}\right)} dy \\
&\quad + \int_{c(\zeta)}^{\infty}\left\{1-\exp\left(-\frac{3d_i^{\alpha}(1+\zeta P_{\text{T}})}{P_{\text{T}}\epsilon\pi^2 M\delta}\right)\right\} \sum_{j\in\Phi_{\text{T}}\setminus i}\exp\left(-\frac{d_j^{\alpha}y}{P_{\text{T}}}\right) \\
&\quad \times \frac{1}{\frac{P_{\text{T}}}{d_j^{\alpha}}\prod_{k\in\Phi_{\text{T}}\setminus\{i,j\}}\left(1-\frac{d_j^{\alpha}}{d_k^{\alpha}}\right)} dy
\end{aligned} \tag{16}$$

where (a) holds since the generalized chi-square distributed variable $y \triangleq \sum_{j\in\Phi_{\text{T}}\setminus i}\frac{P_{\text{T}}}{d_j^{\alpha}}|H_j|^2 \sim \sum_{j\in\Phi_{\text{T}}\setminus i}\frac{\exp(-\frac{d_j^{\alpha}y}{P_{\text{T}}})}{\frac{P_{\text{T}}}{d_j^{\alpha}}\prod_{k\in\Phi_{\text{T}}\setminus\{i,j\}}\left(1-\frac{d_j^{\alpha}}{d_k^{\alpha}}\right)}$ and $|H_i|^2 \sim \exp(1)$. The slack variable $c(\zeta) \triangleq \frac{\gamma_{\text{th}}(1+(1+\delta)\zeta P_{\text{T}})}{1-\delta\gamma_{\text{th}}}$ is defined for notational simplicity. Taking an expectation over $\zeta$ on the integration result of (16), using the mgf $\mathbb{E}_{\Phi^c_{\text{T}}}[\exp(-s\zeta)] = \mathcal{M}_{\zeta}(s)$, finally gives (15). ■

Emphasized again, TxID cannot always be benefitted from preamble cancellation. There exists a fundamental limit to preamble cancellation capability, since preamble signals can be properly canceled only when they are detected correctly. Therefore, the TxID failure events coming together with preamble mis-detection should be counted as well. We accordingly find the joint probability of TxID and

[7] Precisely, if the co-channel interference term is taken into account, the comparison between the robustness of TxID and preamble signals should be obtained by comparing $\frac{3(1+\zeta P_{\text{T}})}{\epsilon\pi^2 M\delta P_{\text{T}}}$ or $\frac{3(1+\zeta P_{\text{T}})}{(\epsilon\pi^2 M\delta-6)P_{\text{T}}}$ with $\frac{\gamma_{\text{th}}(1+(1+\delta)\zeta P_{\text{T}})}{(1-\delta\gamma_{\text{th}})P_{\text{T}}}$. However, unfortunately, randomness and intractability of $\zeta$ entangle categorizing the scenarios concisely. Therefore, the configurations in range of $\frac{\gamma_{\text{th}}}{1-\delta\gamma_{\text{th}}} \leq \frac{3}{\epsilon\pi^2 M\delta} < \frac{3}{\epsilon\pi^2 M\delta-6} < \frac{(1+\delta)\gamma_{\text{th}}}{1-\delta\gamma_{\text{th}}}$ are not considered in this paper, in order to remove $\zeta$ component at declaring scenario condition.

preamble detection failures as

$$\begin{aligned}&\Pr[\sigma^2_{i,\tau}(\mathcal{E})\geq\epsilon,\,\gamma_{\rm p}<\gamma_{\rm th}|\Phi_{\rm T},\mathcal{S}_1]\\&=\Pr\Bigg[\frac{P_{\rm T}}{d_i^{\alpha}}|H_i|^2\leq\min\Bigg\{\frac{1}{\epsilon\pi^2M\delta-6}\Bigg(\sum_{j\in\Phi_{\rm T}\setminus i}\frac{6P_{\rm T}}{d_j^{\alpha}}|H_j|^2+3(1+\zeta P_{\rm T})\Bigg),\\&\quad-\sum_{j\in\Phi_{\rm T}\setminus i}\frac{P_{\rm T}}{d_j^{\alpha}}|H_j|^2+\frac{(1+(1+\delta)\zeta P_{\rm T})\gamma_{\rm th}}{1-\delta\gamma_{\rm th}}\Bigg\}\Bigg]\\&\overset{(a)}{=}\Pr\Bigg[\frac{P_{\rm T}}{d_i^{\alpha}}|H_i|^2\leq-\sum_{j\in\Phi_{\rm T}\setminus i}\frac{P_{\rm T}}{d_j^{\alpha}}|H_j|^2+\frac{(1+(1+\delta)\zeta P_{\rm T})\gamma_{\rm th}}{1-\delta\gamma_{\rm th}}\Bigg]\end{aligned}\tag{17}$$

for Scenario 1, where (a) owes to the given inequality $\frac{3}{\epsilon\pi^2M\delta}\geq\frac{(1+\delta)\gamma_{\rm th}}{1-\delta\gamma_{\rm th}}$. In Scenario 1, we here find from (a) that preamble detection failure is strictly a subset of TxID failures, underlining that ToC is set to make preambles more robust than TxID signals. In consequence, taking an expectation over $\zeta$ on the cumulative distribution function (cdf) of $\sum_{i\in\Phi_{\rm T}}\frac{P_{\rm T}}{d_i^{\alpha}}|H_i|^2$, which is a cdf of generalized chi-square distribution up to $\frac{(1+(1+\delta)\zeta P_{\rm T})\gamma_{\rm th}}{1-\delta\gamma_{\rm th}}$, gives us the following theorem.

*Theorem 3*: *Within Scenario 1, TxID failure is subordinate to the failure of preamble cancellation, so that gives*

$$\begin{aligned}&\Pr[\sigma^2_{i,\tau}(\mathcal{E})\geq\epsilon,\,\gamma_{\rm p}<\gamma_{\rm th}|\Phi_{\rm T},\mathcal{S}_1]\\&=1-\sum_{i\in\Phi_{\rm T}}\exp\Bigg(-\frac{d_i^{\alpha}\gamma_{\rm th}}{P_{\rm T}(1-\delta\gamma_{\rm th})}\Bigg)\frac{\mathcal{M}_{\zeta}\Big(\frac{d_i^{\alpha}(1+\delta)\gamma_{\rm th}}{1-\delta\gamma_{\rm th}}\Big)}{\prod_{j\in\Phi_{\rm T}\setminus i}\Big(1-\frac{d_i^{\alpha}}{d_j^{\alpha}}\Big)}\end{aligned}\tag{18}$$

*for a given set of* $\Phi_T$.

Combining (15) with (18) therefore provides the net TDFP (19), shown at the bottom of this page.

One can also remark that allocating more power to TxID signals, i.e., assigning greater $\delta$, degrades the quality of service (QoS) of host signals [33]. Such QoS penalty directly degrades the *guaranteed throughput* $\log(1+\gamma_{\rm th})\Pr[\gamma_{\rm p}\geq\gamma_{\rm th}|\Phi_{\rm T}]$, the transmission rate achievable at least, where the threshold SINR of payloads is used to be greater than that of preamble $\gamma_{\rm th}$ [7]. FIGURE 3 shows the impact of $\delta$ on $\Pr[\gamma_{\rm p}\geq\gamma_{\rm th}|\Phi_{\rm T}]$ and $\log(1+\gamma_{\rm th})\Pr[\gamma_{\rm p}\geq\gamma_{\rm th}|\Phi_{\rm T}]$. On the contrary, the behavior of TDFP is unclear since $\Pr[\sigma^2_{i,\tau}(\mathcal{C})\geq\epsilon,\gamma_{\rm p}\geq\gamma_{\rm th}|\Phi_{\rm T},\mathcal{S}_1]$ decreases while $\Pr[\sigma^2_{i,\tau}(\mathcal{E})\geq\epsilon,\gamma_{\rm p}<\gamma_{\rm th}|\Phi_{\rm T},\mathcal{S}_1]=\Pr[\gamma_{\rm p}<\gamma_{\rm th}|\Phi_{\rm T}]$ increases by $\delta$ at the same time. However, with sufficiently large $\epsilon\pi^2M$, the Scenario 1 condition $\frac{3}{\epsilon\pi^2M\delta}\geq\frac{(1+\delta)\gamma_{\rm th}}{1-\delta\gamma_{\rm th}}$ ensures significantly low $\delta\gamma_{\rm th}$ so that makes $\Pr[\sigma^2_{i,\tau}(\mathcal{E})\geq\epsilon,\gamma_{\rm p}<\gamma_{\rm th}|\Phi_{\rm T},\mathcal{S}_1]$ vary by

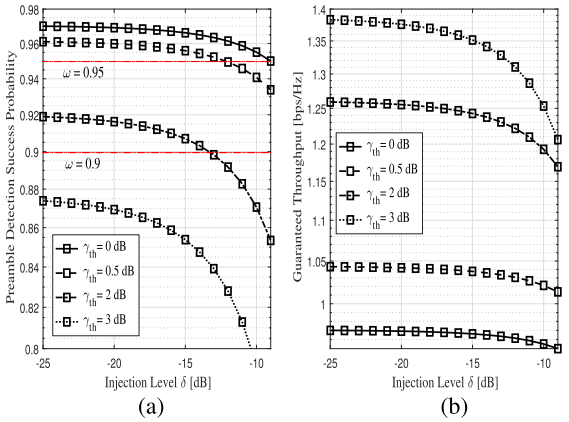


(a) (b)

**FIGURE 3.** **(a) $\Pr[\gamma_{\rm p}\geq\gamma_{\rm th}|\Phi_{\rm T}]$, (b) $\log(1+\gamma_{\rm th})\Pr[\gamma_{\rm p}\geq\gamma_{\rm th}|\Phi_{\rm T}]$ vs. injection level $\delta$ ($P_{\rm T}=120$ dB, $\epsilon=1$, $\alpha=3.5$, $\kappa=1/\pi/1000^2$ [m$^{-2}$], $T=3$, $\{d_1,d_2,d_3\}=\{1000,1500,2000\}$ [m], $r_0=4000$ [m]).**

$\delta$ merely, consequently allowing the TDFP (19) be monotonically decreasing over $\delta$. Note that Scenario 1 condition is equivalent to $\delta\gamma_{\rm th}\leq\frac{3}{(1+\delta)\epsilon\pi^2M+3}\approx\frac{3}{\epsilon\pi^2M}$. Therefore, a TDFP minimization problem which guarantees at least $\exists\omega>0$ success probability for preamble detection

$$\begin{aligned}&\min_{\delta}\Pr[\sigma^2_{i,\tau}\geq\epsilon|\Phi_{\rm T},\mathcal{S}_1]\\&\text{s.t.}\,\Pr[\gamma_{\rm p}\geq\gamma_{\rm th}|\Phi_{\rm T}]\geq\omega\end{aligned}\tag{20}$$

becomes approximately equivalent to the problem searching the maximum $\delta$ in the range of $(0,\min(1,\frac{1}{\gamma_{\rm th}},-\frac{1}{2}-\frac{3}{2\epsilon\pi^2M}+\frac{1}{2}\sqrt{(1+\frac{3}{\epsilon\pi^2M})^2+\frac{12}{\epsilon\pi^2M\gamma_{\rm th}}}))$ subjected to $\Pr[\gamma_{\rm p}\geq\gamma_{\rm th}]\geq\omega$. Besides, the hypergeometric function terms inside the mgfs in (18) let the problem intractable. The solution of (20) hence cannot be derived in closed-form, but can be provided by one-dimensional numerical search over possible $\delta$s.

### 2) SCENARIO 2 ($\mathcal{S}_2$): TxID SIGNAL MORE ROBUST THAN PREAMBLE ($\frac{3}{\epsilon\pi^2M\delta-6}<\frac{\gamma_{\rm th}}{1-\delta\gamma_{\rm th}}$)

As once revealed in the previous part of this subsection, the SIC error propagation could allow the preamble cancellation rather to degrade TxID detection when the Rx fails at detecting preamble signals. If the transmission parameters are predefined in the range of $\frac{3}{\epsilon\pi^2M\delta}\geq\frac{\gamma_{\rm th}}{1-\delta\gamma_{\rm th}}$ however, it is impossible to fail at detecting preamble signals as long as TxID is successfully accomplished. Therefore, we here consider the possible penalty due to mis-cancellations of preamble signals by addressing the scenario TxID signal is set

$$\begin{aligned}\Pr[\sigma^2_{i,\tau}\geq\epsilon|\Phi_{\rm T},\mathcal{S}_1]=1-\exp\Bigg(-\frac{3d_i^{\alpha}}{P_{\rm T}\epsilon\pi^2M\delta}\Bigg)\mathcal{M}_{\zeta}\Bigg(-\frac{3d_i^{\alpha}}{\epsilon\pi^2M\delta}\Bigg)+\sum_{j\in\Phi_{\rm T}\setminus i}\exp\Bigg(-\frac{d_i^{\alpha}\gamma_{\rm th}}{P_{\rm T}(1-\delta\gamma_{\rm th})}\Bigg)\frac{2\mathcal{M}_{\zeta}\Big(\frac{d_i^{\alpha}(1+\delta)\gamma_{\rm th}}{1-\delta\gamma_{\rm th}}\Big)}{(\frac{d_i^{\alpha}}{d_j^{\alpha}}-1)\prod_{k\in\Phi_{\rm T}\setminus\{i,j\}}\Big(1-\frac{d_j^{\alpha}}{d_k^{\alpha}}\Big)}\\-\sum_{j\in\Phi_{\rm T}\setminus i}\exp\Bigg(-\frac{d_j^{\alpha}\gamma_{\rm th}}{P_{\rm T}(1-\delta\gamma_{\rm th})}\Bigg)\frac{2\mathcal{M}_{\zeta}\Big(\frac{d_j^{\alpha}(1+\delta)\gamma_{\rm th}}{1-\delta\gamma_{\rm th}}\Big)}{\Big(\frac{d_i^{\alpha}}{d_j^{\alpha}}-1\Big)\prod_{k\in\Phi_{\rm T}\setminus\{i,j\}}\Big(1-\frac{d_j^{\alpha}}{d_k^{\alpha}}\Big)}\end{aligned}\tag{19}$$

more robust than preamble signal. The conditioning approach likewise to Theorem 2 and Throrem 3 comprehensively gives the TDFP in Scenario 2 by following theorem:

*Theorem 4*: *Given* $\frac{3}{\epsilon\pi^2 M\delta-6} < \frac{\gamma_{th}}{1-\delta\gamma_{th}}$ *and* $\Phi_T$, *the TDFP is given by (21), as shown at the bottom of this page.*

*Proof:* Recall (a) in the equation (16). In case that $\frac{3}{\epsilon\pi^2 M\delta} < \frac{3}{\epsilon\pi^2 M\delta-6} < \frac{\gamma_{\rm th}}{1-\delta\gamma_{\rm th}}$ holds, the range of $-\sum_{j\in\Phi_{\rm T}\setminus i}\frac{P_{\rm T}}{d_j^\alpha}|H_j|^2$ so that there exists $|H_i|^2$ which satisfies the inequality is reduced. Therefore, we have

$$\begin{aligned}
&\Pr[\sigma^2_{i,\tau}(\mathcal{C})\geq\epsilon,\,\gamma_{\rm p}\geq\gamma_{\rm th}|\Phi_{\rm T},\,\Phi_{\rm T}^c,\,\mathcal{S}_2]\\
&=\Pr\Bigg[-\sum_{j\in\Phi_{\rm T}\setminus i}\frac{P_{\rm T}}{d_j^\alpha}|H_j|^2+\frac{\gamma_{\rm th}(1+(1+\delta)\zeta P_{\rm T})}{1-\delta\gamma_{\rm th}}\leq\frac{P_{\rm T}}{d_i^\alpha}|H_i|^2\\
&\leq\frac{3(1+\zeta P_{\rm T})}{\epsilon\pi^2M\delta}\Bigg]\\
&\overset{(a)}{=}\int_{c'(\zeta)}^{c(\zeta)}\Bigg\{\exp\Bigg(-\frac{d_i^\alpha}{P_{\rm T}}\Bigg(y-\frac{\gamma_{\rm th}(1+(1+\delta)\zeta P_{\rm T})}{1-\delta\gamma_{\rm th}}\Bigg)\Bigg)\\
&\quad-\exp\Bigg(-\frac{3d_i^\alpha(1+\zeta P_{\rm T})}{P_{\rm T}\epsilon\pi^2M\delta}\Bigg)\Bigg\}\sum_{j\in\Phi_{\rm T}\setminus i}\frac{\exp(-\frac{d_j^\alpha y}{P_{\rm T}})}{\frac{P_{\rm T}}{d_j^\alpha}\prod_{k\in\Phi_{\rm T}\setminus\{i,j\}}\left(1-\frac{d_j^\alpha}{d_k^\alpha}\right)}dy\\
&\quad+\int_{c(\zeta)}^{\infty}\Bigg\{1-\exp\Bigg(-\frac{3d_i^\alpha(1+\zeta P_{\rm T})}{P_{\rm T}\epsilon\pi^2M\delta}\Bigg)\Bigg\}\sum_{j\in\Phi_{\rm T}\setminus i}\exp\Bigg(-\frac{d_j^\alpha y}{P_{\rm T}}\Bigg)\\
&\quad\times\frac{1}{\frac{P_{\rm T}}{d_j^\alpha}\prod_{k\in\Phi_{\rm T}\setminus\{i,j\}}\left(1-\frac{d_j^\alpha}{d_k^\alpha}\right)}dy,
\end{aligned}\tag{22}$$

where the difference of (a) against the integration range in (16) comes from the condition $\frac{3}{\epsilon\pi^2M\delta-6} < \frac{\gamma_{\rm th}}{1-\delta\gamma_{\rm th}}$. $c'(\zeta)$ is a slack variable defined as $c'(\zeta)\triangleq\frac{\gamma_{\rm th}}{1-\delta\gamma_{\rm th}}-\frac{3}{\epsilon\pi^2M\delta}$. Similarly, let $\frac{\gamma_{\rm th}}{1-\delta\gamma_{\rm th}}-\frac{3}{\epsilon\pi^2M\delta-6}$ denoted as $c''(\zeta)$. Recalling (17) in the proof of Theorem 3, the joint probability of TxID and preamble detection failures can be written by

$$\begin{aligned}
&\Pr[\sigma^2_{i,\tau}(\mathcal{E})\geq\epsilon,\,\gamma_{\rm p}<\gamma_{\rm th}|\Phi_{\rm T},\,\Phi_{\rm T}^c,\,\mathcal{S}_2]\\
&=\Pr\Bigg[\frac{P_{\rm T}}{d_i^\alpha}|H_i|^2\leq\min\Bigg\{\frac{1}{\epsilon\pi^2M\delta-6}\Bigg(\sum_{j\in\Phi_{\rm T}\setminus i}\frac{6P_{\rm T}}{d_j^\alpha}|H_j|^2\\
&\quad+3(1+\zeta P_{\rm T})\Bigg),-\sum_{j\in\Phi_{\rm T}\setminus i}\frac{P_{\rm T}}{d_j^\alpha}|H_j|^2+\frac{(1+(1+\delta)\zeta P_{\rm T})\gamma_{\rm th}}{1-\delta\gamma_{\rm th}}\Bigg\}\Bigg]\\
&\overset{(a)}{=}\int_0^{c''(\zeta)}\Bigg\{1-\exp\Bigg(-\frac{d_i^\alpha}{P_{\rm T}}\Bigg(-\frac{6}{\epsilon\pi^2M\delta-6}y+\frac{3(1+\zeta P_{\rm T})}{\epsilon\pi^2M\delta-6}\Bigg)\Bigg)\Bigg\}\\
&\quad\times\sum_{j\in\Phi_{\rm T}\setminus i}\frac{\exp(-\frac{d_j^\alpha y}{P_{\rm T}})}{\frac{P_{\rm T}}{d_j^\alpha}\prod_{k\in\Phi_{\rm T}\setminus\{i,j\}}\left(1-\frac{d_j^\alpha}{d_k^\alpha}\right)}dy\\
&\quad+\int_{c''(\zeta)}^{c(\zeta)}\Bigg\{1-\exp\Bigg(-\frac{d_i^\alpha}{P_{\rm T}}\Bigg(-y+\frac{\gamma_{\rm th}(1+(1+\delta)\zeta P_{\rm T})}{1-\delta\gamma_{\rm th}}\Bigg)\Bigg)\Bigg\}\\
&\quad\times\sum_{j\in\Phi_{\rm T}\setminus i}\frac{\exp(-\frac{d_j^\alpha y}{P_{\rm T}})}{\frac{P_{\rm T}}{d_j^\alpha}\prod_{k\in\Phi_{\rm T}\setminus\{i,j\}}\left(1-\frac{d_j^\alpha}{d_k^\alpha}\right)}dy.
\end{aligned}\tag{23}$$

The limitation $c''(\zeta)$ in (a) comes from the comparison between $\frac{1}{\epsilon\pi^2M\delta-6}(6y+3(1+\zeta P_{\rm T}))$ and $-y+\frac{(1+(1+\delta)\zeta P_{\rm T})\gamma_{\rm th}}{1-\delta\gamma_{\rm th}}$. Subsequently, obtaining expectation on the sum of (22) and (23) over $\zeta$ gives (21) so that concludes the proof. ■

The integration range of $y$ in (a) is reduced compared to that in (b) in (16). That is, having the signal parameter configuration $\frac{3}{\epsilon\pi^2M\delta-6} < \frac{\gamma_{\rm th}}{1-\delta\gamma_{\rm th}}$, the TxID detector falls into preamble outage frequently than $\frac{3}{\epsilon\pi^2M\delta} \geq \frac{\gamma_{\rm th}(1+\delta)}{1-\delta\gamma_{\rm th}}$ during TxID detection is in outage. On the contrary, more $y$s are covered in the integration in (b) of (23) than (a) of (17). It also reveals that TxID detection failure event is more occurred with preamble detection failure in Scenario 2 than Scenario 1.

Scenario 2 on contrary to Scenario 1, the TDFP can be way more affected by preamble detection failures. The mis-cancellation further adds additional penalty to TxID signal detection. This degradation is reflected to the drastic increase of TDFP in FIGURE 4. Note also from FIGURE 3 that $\Pr[\gamma_{\rm p}\geq\gamma_{\rm th}|\Phi_{\rm T}]$ becomes considerably low for $\gamma_{\rm th}$s over 3 dB. Notable amount of preamble mis-cancellation occurs in this $\gamma_{\rm th}$ region, so that would even degrade the performance of PCTD than CTD. The point of transition between Scenario 1 and Scenario 2 should be also highlighted. Where the available $\delta$ in Scenario 1 is limited up

$$\begin{aligned}
&\Pr[\sigma^2_{i,\tau}\geq\epsilon|\Phi_{\rm T},\,\mathcal{S}_2]\\
&=1+\sum_{j\in\Phi_{\rm T}\setminus i}\exp\Bigg(-\frac{d_j^\alpha\gamma_{\rm th}}{P_{\rm T}(1-\delta\gamma_{\rm th})}\Bigg)\frac{\frac{d_i^\alpha}{d_j^\alpha}\mathcal{M}_\zeta\left(\frac{d_j^\alpha(1+\delta)\gamma_{\rm th}}{1-\delta\gamma_{\rm th}}\right)}{\left(\frac{d_i^\alpha}{d_j^\alpha}-1\right)\prod_{k\in\Phi_{\rm T}\setminus\{i,j\}}\left(1-\frac{d_j^\alpha}{d_k^\alpha}\right)}-\sum_{j\in\Phi_{\rm T}\setminus i}\exp\Bigg(-\frac{d_j^\alpha\gamma_{\rm th}}{P_{\rm T}(1-\delta\gamma_{\rm th})}-\frac{3(d_i^\alpha-d_j^\alpha)}{P_{\rm T}\epsilon\pi^2M\delta}\Bigg)\frac{\frac{d_i^\alpha}{d_j^\alpha}\mathcal{M}_\zeta\left(\frac{d_j^\alpha\gamma_{\rm th}}{1-\delta\gamma_{\rm th}}+\frac{3(d_i^\alpha-d_j^\alpha)}{\epsilon\pi^2M\delta}\right)}{\left(\frac{d_i^\alpha}{d_j^\alpha}-1\right)\prod_{k\in\Phi_{\rm T}\setminus\{i,j\}}\left(1-\frac{d_j^\alpha}{d_k^\alpha}\right)}\\
&\quad-\sum_{j\in\Phi_{\rm T}\setminus i}\exp\Bigg(-\frac{3d_i^\alpha}{P_{\rm T}(\epsilon\pi^2M\delta-6)}\Bigg)\frac{\mathcal{M}_\zeta\left(-\frac{3d_i^\alpha}{\epsilon\pi^2M\delta-6}\right)}{\left(\frac{6d_i^\alpha}{d_j^\alpha(\epsilon\pi^2M\delta-6)}+1\right)\prod_{k\in\Phi_{\rm T}\setminus\{i,j\}}\left(1-\frac{d_j^\alpha}{d_k^\alpha}\right)}-\sum_{j\in\Phi_{\rm T}\setminus i}\exp\Bigg(-\frac{d_j^\alpha\gamma_{\rm th}}{P_{\rm T}(1-\delta\gamma_{\rm th})}\Bigg)\frac{\frac{d_i^\alpha}{d_j^\alpha}\mathcal{M}_\zeta\left(\frac{d_j^\alpha(1+\delta)\gamma_{\rm th}}{1-\delta\gamma_{\rm th}}\right)}{\left(\frac{d_i^\alpha}{d_j^\alpha}-1\right)\prod_{k\in\Phi_{\rm T}\setminus\{i,j\}}\left(1-\frac{d_j^\alpha}{d_k^\alpha}\right)}\\
&\quad+\sum_{j\in\Phi_{\rm T}\setminus i}\exp\Bigg(\frac{3d_i^\alpha\left(\frac{2\gamma_{\rm th}}{1-\delta\gamma_{\rm th}}+1\right)}{P_{\rm T}\epsilon\pi^2M\delta}-\frac{d_j^\alpha\left(\frac{\gamma_{\rm th}}{1-\delta\gamma_{\rm th}}-\frac{3}{\epsilon\pi^2M\delta-6}\right)}{P_{\rm T}\left(\frac{6}{\epsilon\pi^2M\delta-6}+1\right)}\Bigg)\frac{\mathcal{M}_\zeta\left(-\frac{3d_i^\alpha\left(\frac{2(1+\delta)\gamma_{\rm th}}{1-\delta\gamma_{\rm th}}+1\right)}{P_{\rm T}\epsilon\pi^2M\delta}-\frac{d_j^\alpha\left(\frac{(1+\delta)\gamma_{\rm th}}{1-\delta\gamma_{\rm th}}-\frac{3}{\epsilon\pi^2M\delta-6}\right)}{P_{\rm T}\left(\frac{6}{\epsilon\pi^2M\delta-6}+1\right)}\right)}{\left(\frac{6d_i^\alpha}{d_j^\alpha(\epsilon\pi^2M\delta-6)}+1\right)\left(\frac{d_i^\alpha}{d_j^\alpha}-1\right)\prod_{k\in\Phi_{\rm T}\setminus\{i,j\}}\left(1-\frac{d_j^\alpha}{d_k^\alpha}\right)}
\end{aligned}\tag{21}$$

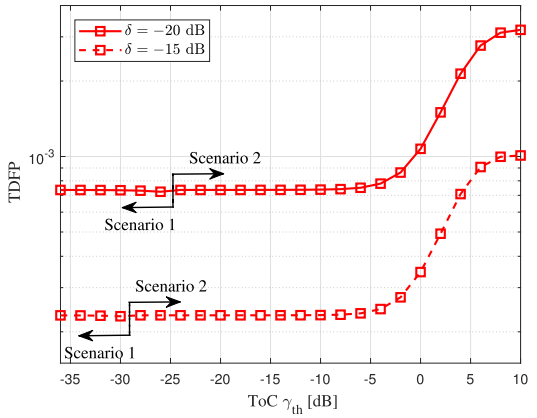


**FIGURE 4.** TDFP vs. ToC $\gamma_{\text{th}}$ ($P_{\text{T}} = 120$ dB, $\epsilon = 1$, $M = 8191$, $\alpha = 3.5$, $\kappa = 1/\pi/1000^2$ [m$^{-2}$], $T = 3$, $\{d_1, d_2, d_3\} = \{1000, 1500, 2000\}$ [m], $r_0 = 4000$ [m]).

to $\min(\frac{1}{\delta}, \frac{3}{\delta((1+\delta)\epsilon\pi^2 M+3)})$ while the lowest $\gamma_{\text{th}}$ allowed in Scenario 2 is $(\delta+\frac{\epsilon\pi^2 M\delta-6}{3})^{-1}$, the higher $\delta$ reduces the portion of Scenario 1. The constrained TDFP minimization problem in (20) can be expanded to $\min_\delta \Pr[\sigma^2_{i,\tau} \geq \epsilon|\Phi_{\text{T}}, \mathcal{S}_1 \text{ or } \mathcal{S}_2]$ s.t. $\Pr[\gamma_{\text{p}} \geq \gamma_{\text{th}}|\Phi_{\text{T}}]$ with regarding Scenario 2 also, and can be solved by one-dimensional search within limited range of $\delta \in (0, \min(1, \frac{1}{\gamma_{\text{th}}}, -\frac{1}{2}-\frac{3}{2\epsilon\pi^2 M}+\frac{1}{2}\sqrt{(1+\frac{3}{\epsilon\pi^2 M})^2+\frac{12}{\epsilon\pi^2 M\gamma_{\text{th}}}})) \cup (\frac{3+6\gamma_{\text{th}}}{\gamma_{\text{th}}(\epsilon\pi^2 M+3)}, \min(1, \frac{1}{\gamma_{\text{th}}}))$.

*Remark (PCTD in High Co-Channel Interference Environment):* On the other hand, there is another remark on the effectiveness of PCTD. A simple conditioning allows us to express TDFP by $\Pr[\sigma^2_{i,\tau} \geq \epsilon|\Phi_{\text{T}}, \text{PCTD}] = \Pr[\sigma^2_{i,\tau}(\mathcal{E}) \geq \epsilon|\Phi_{\text{T}}, \gamma_{\text{p}} < \gamma_{\text{th}}] - \Pr[\gamma_{\text{p}} \geq \gamma_{\text{th}}](\Pr[\sigma^2_{i,\tau}(\mathcal{E}) \geq \epsilon|\Phi_{\text{T}}, \gamma_{\text{p}} < \gamma_{\text{th}}] - \Pr[\sigma^2_{i,\tau}(\mathcal{C}) \geq \epsilon|\Phi_{\text{T}}, \gamma_{\text{p}} \geq \gamma_{\text{th}}])$. This expression implies that the preamble cancellation advantages from the difference of $\Pr[\sigma^2_{i,\tau}(\mathcal{E}) \geq \epsilon|\Phi_{\text{T}}, \gamma_{\text{p}} < \gamma_{\text{th}}]$ and $\Pr[\sigma^2_{i,\tau}(\mathcal{C}) \geq \epsilon|\Phi_{\text{T}}, \gamma_{\text{p}} \geq \gamma_{\text{th}}]$. However, when co-channel interference dominates the signals from Txs in $\Phi_{\text{T}}$, this gap shrinks into zero since $\sigma^2_{i,\tau}(\mathcal{E})$ converges into $\sigma^2_{i,\tau}(\mathcal{C})$. PCTD is thus inferred to be less preferable for highly dense $\Phi^c_{\text{T}}$ environments. Furthermore, the superiority of $\sigma^2_{i,\tau}(\mathcal{E})$ to the CRB of CTD (3) implies that CTD would be rather desirable than PCTD in high co-channel interference environments.

### C. OPPORTUNISTIC PREAMBLE CANCELLATION (OPC)

One simple strategy to avoid such error propagation penalty is OPC. As previously been discussed, it is obvious that the basic TxID detection without canceling preamble is rather beneficial when preamble cannot be detected successfully. Therefore, enabling the preamble cancellation process only when the preamble is successfully decoded, as FIGURE 5, will minimize the detection failure occurrence. OPC is feasible in practice since the TxID detector would possibly run a decoding error check on preamble signals, such as a syndrome check calculation. When OPC is applied, the TDFP is given by (24), as shown at the bottom of this page, for Scenario 2.[8] On the contrary, in case of Scenario 1, OPC does not reduce the TDFP from (19) since preamble detection failure is sufficient for TxID detection failure when $\frac{3}{\epsilon\pi^2 M\delta} \geq \frac{\gamma_{\text{th}}(1+\delta)}{1-\delta\gamma_{\text{th}}}$ holds.

## V. NUMERICAL RESULTS

In this section, the detection failure performance of RF-watermark type TxID is verified by numerical calculation based on the results in Section III and IV. Our analytic model is first validated through empirical simulations in Section V-A and the detection performance gain from preamble cancellation is subsequently verified in Section V-B. Throughout this section, three-Tx SFN (i.e., $T = 3$) is considered, where the distances from the Rx are set to $\{d_1, d_2, d_3\} = \{1000, 1500, 2000\}$ m and the guard distance is given $r_0 = 4000$ m, motivated by the recent ATSC 3.0 SFN installation in South Korea [34]. The preamble transmission power at each Tx is given $P_{\text{T}} = 120$ dB. Additionally, the length of TxID sequence was assumed $M = 8191$ [9]referring to ATSC 3.0 physical layer protocol.

[8](24) can be straightforwardly obtained from the result and proof of Theorem 4.

[9]It refers to ATSC 3.0 physical layer standard [14]. ATSC 3.0 uses a Gold type PN sequence with a length of 8191 for TxID.

$$
\begin{aligned}
&\Pr[\sigma^2_{i,\tau} \geq \epsilon|\Phi_{\text{T}}, \mathcal{S}_2, OPC] \\
&= 1+\sum_{j\in\Phi_{\text{T}}\setminus i}\exp\left(-\frac{d_j^\alpha\gamma_{\text{th}}}{P_{\text{T}}(1-\delta\gamma_{\text{th}})}\right)\frac{\frac{d_i^\alpha}{d_j^\alpha}\mathcal{M}_\zeta\left(\frac{d_j^\alpha(1+\delta)\gamma_{\text{th}}}{1-\delta\gamma_{\text{th}}}\right)}{\left(\frac{d_i^\alpha}{d_j^\alpha}-1\right)\prod_{k\in\Phi_{\text{T}}\setminus\{i,j\}}\left(1-\frac{d_j^\alpha}{d_k^\alpha}\right)} - \sum_{j\in\Phi_{\text{T}}\setminus i}\exp\left(-\frac{d_j^\alpha\gamma_{\text{th}}}{P_{\text{T}}(1-\delta\gamma_{\text{th}})}-\frac{3(d_i^\alpha-d_j^\alpha)}{P_{\text{T}}\epsilon\pi^2 M\delta}\right)\frac{\frac{d_i^\alpha}{d_j^\alpha}\mathcal{M}_\zeta\left(\frac{d_j^\alpha\gamma_{\text{th}}}{1-\delta\gamma_{\text{th}}}+\frac{3(d_i^\alpha-d_j^\alpha)}{\epsilon\pi^2 M\delta}\right)}{\left(\frac{d_i^\alpha}{d_j^\alpha}-1\right)\prod_{k\in\Phi_{\text{T}}\setminus\{i,j\}}\left(1-\frac{d_j^\alpha}{d_k^\alpha}\right)} \\
&\quad -\sum_{j\in\Phi_{\text{T}}\setminus i}\exp\left(-\frac{3d_i^\alpha}{P_{\text{T}}(\epsilon\pi^2 M\delta-3)}\right)\frac{\mathcal{M}_\zeta\left(-\frac{3d_i^\alpha}{\epsilon\pi^2 M\delta-3}\right)}{\left(\frac{3d_i^\alpha}{d_j^\alpha(\epsilon\pi^2 M\delta-3)}+1\right)\prod_{k\in\Phi_{\text{T}}\setminus\{i,j\}}\left(1-\frac{d_j^\alpha}{d_k^\alpha}\right)} - \sum_{j\in\Phi_{\text{T}}\setminus i}\exp\left(-\frac{d_j^\alpha\gamma_{\text{th}}}{P_{\text{T}}(1-\delta\gamma_{\text{th}})}\right)\frac{\frac{d_i^\alpha}{d_j^\alpha}\mathcal{M}_\zeta\left(\frac{d_j^\alpha(1+\delta)\gamma_{\text{th}}}{1-\delta\gamma_{\text{th}}}\right)}{\left(\frac{d_i^\alpha}{d_j^\alpha}-1\right)\prod_{k\in\Phi_{\text{T}}\setminus\{i,j\}}\left(1-\frac{d_j^\alpha}{d_k^\alpha}\right)} \\
&\quad +\sum_{j\in\Phi_{\text{T}}\setminus i}\exp\left(-\frac{3d_i^\alpha\left(\frac{2\gamma_{\text{th}}}{1-\delta\gamma_{\text{th}}}+1\right)}{P_{\text{T}}\epsilon\pi^2 M\delta}-\frac{d_j^\alpha\left(\frac{\gamma_{\text{th}}}{1-\delta\gamma_{\text{th}}}-\frac{3}{\epsilon\pi^2 M\delta-3}\right)}{P_{\text{T}}\left(\frac{3}{\epsilon\pi^2 M\delta-3}+1\right)}\right)\frac{\mathcal{M}_\zeta\left(-\frac{3d_i^\alpha\left(\frac{2(1+\delta)\gamma_{\text{th}}}{1-\delta\gamma_{\text{th}}}+1\right)}{P_{\text{T}}\epsilon\pi^2 M\delta}-\frac{d_j^\alpha\left(\frac{(1+\delta)\gamma_{\text{th}}}{1-\delta\gamma_{\text{th}}}-\frac{3}{\epsilon\pi^2 M\delta-3}\right)}{P_{\text{T}}\left(\frac{3}{\epsilon\pi^2 M\delta-3}+1\right)}\right)}{\left(\frac{3d_i^\alpha}{d_j^\alpha(\epsilon\pi^2 M\delta-3)}+1\right)\left(\frac{d_i^\alpha}{d_j^\alpha}-1\right)\prod_{k\in\Phi_{\text{T}}\setminus\{i,j\}}\left(1-\frac{d_j^\alpha}{d_k^\alpha}\right)}
\end{aligned}
\tag{24}
$$

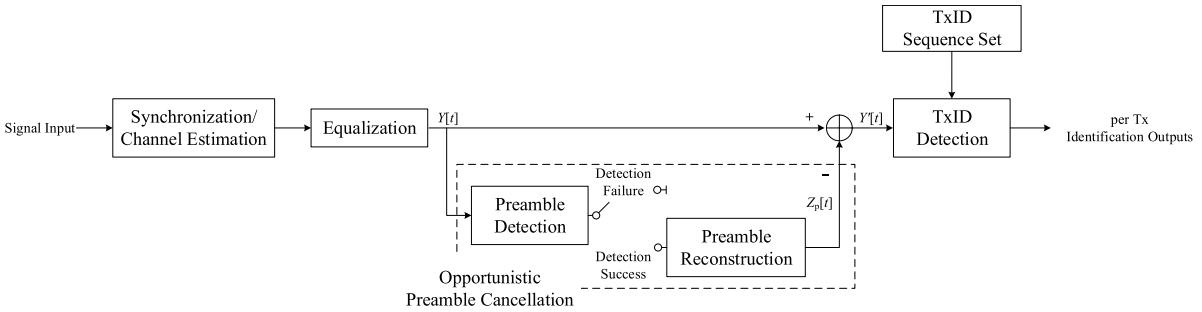


**FIGURE 5.** Block diagram of opportunistic preamble cancellation procedure.

### A. FEASIBILITY OF TDFP DERIVATIONS

Before turning to quantify the preamble cancellation gain on TDFP, the feasibility of our analytic results were first investigated. To this end, Monte Carlo simulations over several $10^6$ iterations were conducted, within the Rx-centered disk having a radius of $10^5$ m. The TDFP of CTD, particularly, was addressed for this validation, where the expressions for PCTD are basically formed as a weighted sum-expansion of the TDFP formula of CTD. As notified in FIGURE 6, $\alpha$ of 3.5 was used, and the interfering Txs were distributed with $\kappa = 1/\pi/1000^2$ m$^{-2}$ throughout the simulations.

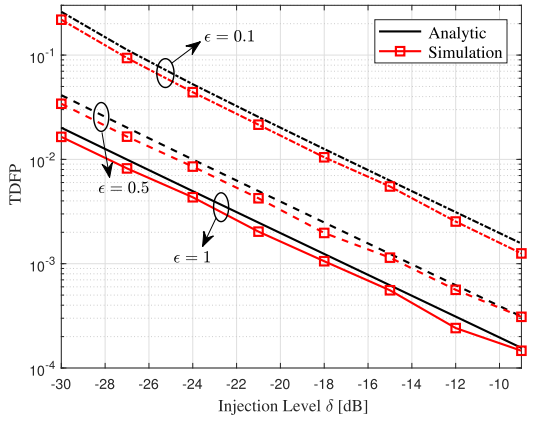


**FIGURE 6.** TDFP of CTD vs. injection level $\delta$ ($\epsilon \in \{0.1, 0.5, 1\}$, $\alpha = 3.5$, $\kappa = 1/\pi/1000^2$ [m$^{-2}$]).

In FIGURE 6, the analytic result in (9) was first found to align with the empirical results well. For example, (9) was $1.0 \times 10^{-4}$ apart from the simulation result for $(\delta, \epsilon) = (-15$ dB, $0.5)$ case. Can be noticed, the gap between simulation and analytic results can be better tightened when the simulations within geometrically larger area (taking more interferer Txs into account) are conducted. Meantime, TDFP came increased under more rigorous precision criterion, i.e., lower $\epsilon$. Moreover, the monotonic decreasing tendency of TDFP over $\delta$ was also observed in FIGURE 6. This tendency comes along with the discussion in Section III, the monotonicity reasoning for CTD.

### B. PERFORMANCE OF PCTD

Through comparisons with the conventional TxID detector, the detection performance gain attained from preamble

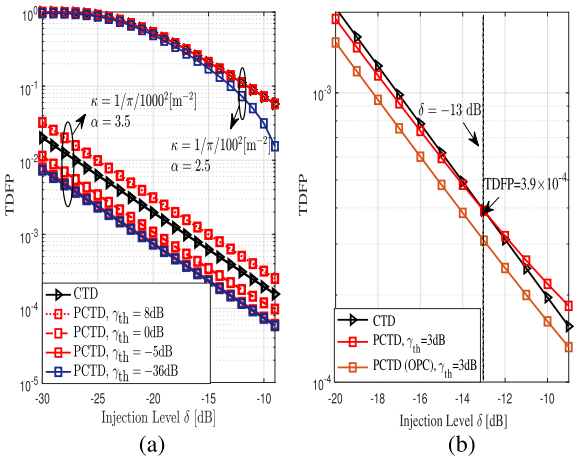


**FIGURE 7.** TDFP (a) without OPC, (b) with OPC vs. injection level $\delta$ ($\epsilon = 1$, $\alpha = 3.5$, $\kappa = 1/\pi/1000^2$ [m$^{-2}$]).

cancellation was verified in FIGURE 7 - FIGURE 10. Scenario 1 and 2 were both considered for the verification, where the threshold SINR of preamble detection $\gamma_{\text{th}}$ of $-36$ dB was considered for scenario 1 while that of $-5$, 0, 8 dB were considered for scenario 2.

According to FIGURE 7, preamble cancellation was found to substantially reduce TDFP as long as $\gamma_{\text{th}}$ is given low enough. For $\kappa = 1/\pi/1000^2$ m$^{-2}$, $\alpha = 3.5$ case in FIGURE 7(a), the scenario 1 preamble cancellation provided over 4 dB injection level gain compared to CTD, where the performance gain was shown in the entire injection level region considered. Since a failure at preamble detection causes a mis-cancellation when OPC is not considered, more frequent detection failure was observed at the PCTD when $\gamma_{\text{th}}$ was increased. Particularly under $\kappa = 1/\pi/1000^2$ m$^{-2}$, $\alpha = 3.5$, the PCTD attained about 2.5 dB injection level gain in $\gamma_{\text{th}} = 0$ dB case, which is reduced from the injection level gain in the $\gamma_{\text{th}} = -36$ dB case but still outperformed CTD. On the contrary, in $\gamma_{\text{th}} = 8$ dB case, the PCTD required 2 dB higher injection level than CTD for the same TDFP. The crosspoint between the TDFPs of PCTD and CTD in FIGURE 7(b) highlighted this aspect further precisely. The TDFP of PCTD exceeded that of CTD at $\delta = -13$ dB under the ToC of $\gamma_{\text{th}} = 3$ dB, which is the point $\Pr[\gamma_{\text{p}} \geq \gamma_{\text{th}} | \Phi_{\text{T}}]$ in FIGURE 3(a) was found 0.83. As mentioned in Section IV-C in advance, applying OPC meantime overcame the mis-cancellation penalty in practice. The TDFP of OPC in

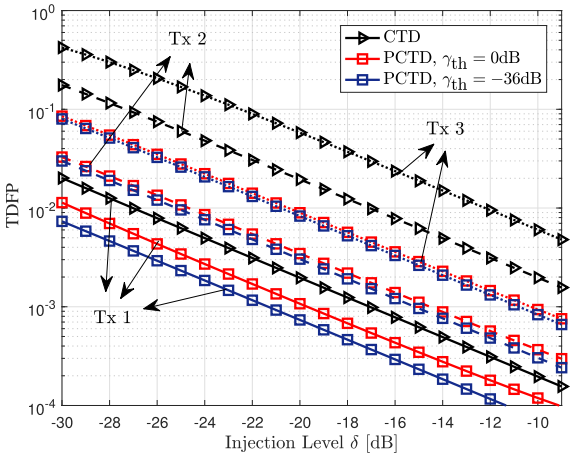


**FIGURE 8.** TDFP vs. injection level $\delta$ ($\epsilon = 1$, $\alpha = 3.5$, $\kappa = 1/\pi/1000^2$ [m$^{-2}$]).

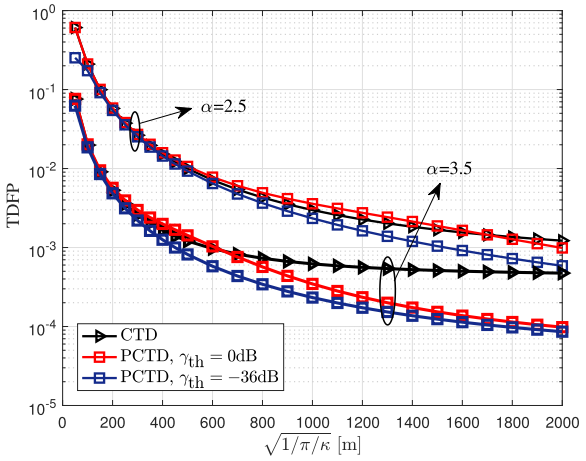


**FIGURE 10.** TDFP vs. $\sqrt{1/\pi/\kappa}$ ($\epsilon = 1$, $\delta = -15$ [dB], $\alpha = 3.5$, $r_0 = 4000$ [m]).

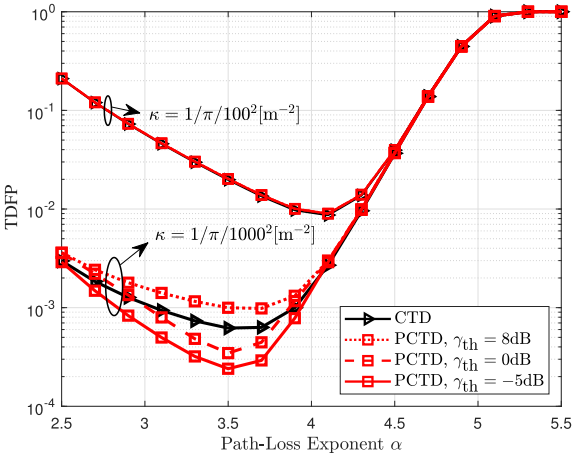


**FIGURE 9.** TDFP vs. path-loss exponent $\alpha$ ($\epsilon = 1$, $\delta = -15$ [dB], $\kappa = 1/\pi/1000^2$ [m$^{-2}$]).

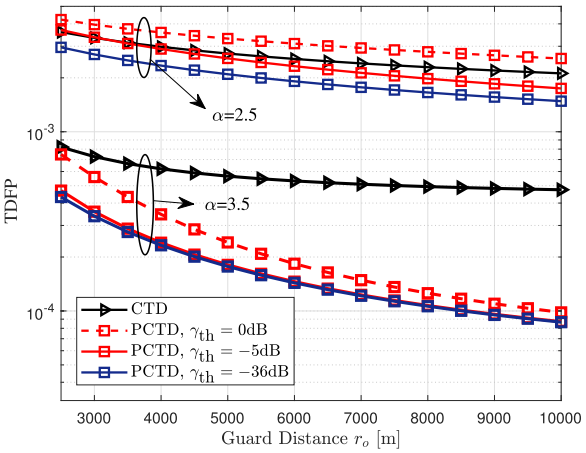


**FIGURE 11.** TDFP vs. guard distance $r_0$ ($\epsilon = 1$, $\delta = -15$ [dB], $\kappa = 1/\pi/1000^2$ [m$^{-2}$], $\alpha = 3.5$).

FIGURE 7(b) was found about 1∼2 dB beneficial than both PCTD and CTD. However, the PCTD was shown effective in reasonable range of $\gamma_{\text{th}}$, where $\gamma_{\text{th}} = -5$ dB[10] case provided analogous performance to $\gamma_{\text{th}} = -36$ dB case.

The detection performance gain from preamble cancellation was found more enhanced for the far Txs. In FIGURE 8 presenting the TDFPs for the TxID of every Txs in $\Phi_{\text{T}}$, the PCTD with $\gamma_{\text{th}} = 0$ dB acquired about 8 dB injection level gain compared to CTD, particularly for an identification of the 2nd close Tx (Tx 2 in short, $d_2 = 1500$ m). Note that the injection level gain from preamble cancellation was about 4 dB for the first close Tx (Tx 1, $d_1 = 1000$ m). Since the aggregated preamble signals disturb the TxID detection more for the far Txs than for the closer Txs, preamble cancellation is especially effective at identifying the far Tx signals.

FIGURE 9 compares the performance of the PCTD and CTD with respect to path-loss exponent $\alpha$. Under $\kappa = 1/\pi/1000^2$ m$^{-2}$, the performances of TxID detection with and without preamble cancellation were shown most diverged at $\alpha = 3.5$, while the performance gap was reduced in low- and high-$\alpha$ region. It is noteworthy to point out that there is a tradeoff between desired signal attenuation and co-channel interference attenuation with regard to $\alpha$. Note that the tradeoff also holds for preamble detection. Therefore, if $\gamma_{\text{th}}$ is fixed, the performance superiority between the PCTD and CTD can be differed depending on $\alpha$. For instance, in $\kappa = 1/\pi/1000^2$ m$^{-2}$ case of FIGURE 9, the PCTD with $\gamma_{\text{th}} = 0$ dB showed lower TDFP than CTD in $2.9 \leq \alpha \leq 3.8$ while CTD showed better detection performance in other $\alpha$ region. It can be reasonably inferred that the PCTD was penalized by a preamble detection failure increase due to less attenuated co-channel interference for $\alpha < 2.9$ region and due to preamble signal power attenuation for $\alpha > 3.8$ region. In contrast to $\kappa = 1/\pi/1000^2$ m$^{-2}$ case, the failure probability gap between the PCTD and CTD was found mere in highly dense interferer network with $\kappa = 1/\pi/100^2$ m$^{-2}$.

The impact of the out-of-guard interval interferers' intensity was also investigated in FIGURE 10. PCTD was observed especially beneficial in low $\kappa$ networks, having 79% reduced

[10]Recall that preamble is a reference signal which is designed to be highly robust to noise and interference in general.

TDFP compared to CTD for $\kappa = 1/\pi/2000^2$ m$^{-2}$ network with $\alpha = 3.5$. The advantage of preamble cancellation in low co-channel interference networks was also demonstrated in FIGURE 11 by a comparison with respect to $r_0$. Under $r_0 = 10000$ m condition, canceling preamble that has $\gamma_{\text{th}} = -5$ dB threshold SINR obtained 82% failure reduction for $\alpha = 3.5$. In contrast, with $\alpha = 2.5$, co-channel interference was not sufficiently attenuated to overcome the detection failure on $\gamma_{\text{th}} = 0$ dB preamble so that the PCTD yielded more frequent failure than CTD in FIGURE 11.

## VI. CONCLUSION

This paper evaluated the CRB-based error performance of the PCTD in SFN with randomly distributed out-of-coverage Txs. The system of interest employed the RF-watermark type TxID signal injected in the host preamble signal, likewise to what is as defined in the ATSC 3.0 protocol. Outage probabilities for TxID detection were derived on the top of the homogeneous PPP-based stochastic geometry framework. Based on the analytic results, the preamble cancellation was revealed to be especially beneficial for far Txs and in low out-of-guard interval interference networks. It was also numerically shown that the preamble cancellation-assisted technique substantially reduces the TxID detection failure, where over 4 dB injection level gain was obtained when the threshold SINR of preamble detection was given $-5$ dB.

## APPENDIX
## CRB-BASED VALIDATION OF THE RESULT IN [1]

The previous study [1] has observed the heuristic gain of PCTD in 2-Tx SFN through computer simulations, laboratory tests, and field experiments. The experiments have been conducted with practical orthogonal frequency division multiplexing (OFDM) realizations, particularly conforming to ATSC 3.0 protocol. The authors of [1] have accordingly claimed that PCTD has about 15∼18 dB of injection level gain over CTD, while the newtork suffers from AWGN channel without fading effect. Where the fading effect has been neglected, the simulation configuration in [1] has set the received SNR to be 15 dB instead of considering the Tx power and path-loss independently. We here show that the empirical result in [1] can be explained in our analytic framework based on CRB.

Let us denote the target CRB by $\sigma_\tau^{*2}$ and the injection levels required to achieve $\sigma_\tau^{*2}$ under CTD and PCTD by $\delta_{\text{CTD}}$ and $\delta_{\text{PCTD}}$, respectively. Note that the experiments in [1] has aimed at the circumstances that preamble signals are successfully detected, where the considered TxID analyzer is a supplemental module mounted in the commercial ATSC 3.0 broadcast Rx, which is available when the Rx attains L1-signal information successfully. Following the definition in (3) and (12), we have $\sigma_\tau^{*2} = \frac{3}{\epsilon\pi^2 M \delta_{\text{PCTD}} P_{\text{Rx}}} = (1+2P_{\text{Rx}})(\frac{\epsilon\pi^2 M \delta_{\text{CTD}} P_{\text{Rx}}}{3})^{-1}$, where $P_{\text{Rx}}$ indicates the received SNR, which is set to be 15 dB. It is reasonably assumed that CTD and PCTD pursues the identical detection precision $\epsilon$. This equality is equivalent to

$$\delta_{\text{CTD}} = \delta_{\text{PCTD}}(1+2P_{\text{Rx}}), \tag{25}$$

which can be approximately rewritten by $\delta_{\text{CTD}} \approx 2\delta_{\text{PCTD}} P_{\text{Rx}}$. Recalling $P_{\text{Rx}} = 15$ dB, the argument in [1], about 18 dB injection level gain of PCTD, is valid for the considered environment.

## REFERENCES

[1] S. Kwon, S.-I. Park, J.-Y. Lee, B.-M. Lim, S. Ahn, and J. Kang, "Detection schemes for ATSC 3.0 transmitter identification in single frequency network," *IEEE Trans. Broadcast.*, early access, Oct. 15, 2019, doi: 10.1109/TBC.2019.2941074.
[2] Y. Wu, B. Rong, K. Salehian, and G. Gagnon, "Cloud transmission: A new spectrum-reuse friendly digital terrestrial broadcasting transmission system," *IEEE Trans. Broadcast.*, vol. 58, no. 3, pp. 329–337, Sep. 2012.
[3] A. Mattsson, "Single frequency networks in DTV," *IEEE Trans. Broadcast.*, vol. 51, no. 4, pp. 413–422, Dec. 2005.
[4] S.-I. Park, J.-Y. Lee, S. Kwon, B.-M. Lim, S. Ahn, H. M. Kim, S. Jeon, J. Lee, M. Simon, M. Aitken, K. Gage, Y. Wu, L. Zhang, W. Li, and J. Kim, "Performance analysis of all modulation and code combinations in ATSC 3.0 physical layer protocol," *IEEE Trans. Broadcast.*, vol. 65, no. 2, pp. 197–210, Jun. 2019.
[5] W. Li, Y. Wu, S. Lafleche, K. Salehian, L. Zhang, A. Florea, S.-I. Park, J.-Y. Lee, H.-M. Kim, N. Hur, C. Regueiro, J. Montalban, and P. Angueira, "Coverage study of ATSC 3.0 under strong co-channel interference environments," *IEEE Trans. Broadcast.*, vol. 65, no. 1, pp. 73–82, Mar. 2019.
[6] S. Ahn, J. Kim, S.-I. Park, J.-Y. Lee, B.-M. Lim, S. Kwon, N. Hur, Y. Wu, L. Zhang, and W. Li, "Mobile performance evaluation for ATSC 3.0 physical layer modulation and code combinations under TU-6 channel," *IEEE Trans. Broadcast.*, early access, Jan. 1, 2020, doi: 10.1109/TBC.2019.2954065.
[7] *ATSC Recommended Practice: A/327, Guidelines for the Physical Layer Protocol*, Advanced Television Systems Committee, document A/327, Oct. 2018.
[8] X. Wang, Y. Wu, and B. Caron, "Transmitter identification using embedded pseudo random sequences," *IEEE Trans. Broadcast.*, vol. 50, no. 3, pp. 244–252, Sep. 2004.
[9] R. L. Peterson, R. E. Ziemer, and D. E. Borth, *Introduction to Spread-Spectrum Communications*. Upper Saddle River, NJ, USA: Prentice-Hall, 1995.
[10] D. Torrieri, *Principles of Spread-Spectrum Communication Systems*. Springer, 2005.
[11] X. Feng, H.-C. Wu, Y. Wu, and X. Wang, "Kasami sequence studies for DTV transmitter identification," *IEEE Trans. Consum. Electron.*, vol. 58, no. 4, pp. 1138–1146, Nov. 2012.
[12] H.-C. Wu and Y. Wu, "Novel robust transmitter identification technique for digital television signals," in *Proc. IEEE Global Commun. Conf. (GLOBECOM)*, Dec. 2013, pp. 3288–3293.
[13] *ATSC Standard: A/111, Design of Synchronized Multiple Transmitter Networks*, Advanced Television Systems Committee, document A/111, Sep. 2009.
[14] *ATSC Standard: A/322, Physical Layer Protocol*, Advanced Television Systems Committee, document A/322, Jun. 2017.
[15] S.-I. Park, W. Li, J.-Y. Lee, Y. Wu, X. Wang, S. Kwon, B.-M. Lim, H. M. Kim, N. Hur, L. Zhang, and J. Kim, "ATSC 3.0 transmitter identification signals and applications," *IEEE Trans. Broadcast.*, vol. 63, no. 1, pp. 240–249, Mar. 2017.
[16] S. Ik Park, J.-Y. Lee, H. Mook Kim, and W. Oh, "Transmitter identification signal analyzer for single frequency network," *IEEE Trans. Broadcast.*, vol. 54, no. 3, pp. 383–393, Sep. 2008.
[17] J. Montalban, E. Iradier, P. Angueira, S.-I. Park, S. Kwon, and N. Hur, "Channel estimation: Key factor for LDM based local content delivery on SFNs," in *Proc. IEEE Int. Symp. Broadband Multimedia Syst. Broadcast. (BMSB)*, Valencia, Spain, Jun. 2018, pp. 1–6.
[18] L. Zhang, W. Li, Y. Wu, S. Lafleche, K. Salehian, Z. Hong, A. Florea, X. Wang, S.-I. Park, H. M. Kim, J.-Y. Lee, N. Hur, P. Angueira, J. Montalban, and C. Regueiro, "Channel estimation strategy for using LDM to deliver local content insertion in ATSC 3.0," in *Proc. IEEE Int. Symp. Broadband Multimedia Syst. Broadcast. (BMSB)*, Cagliari, Italy, Jun. 2017, pp. 1–5.

[19] O. Simeone, Y. Bar-Ness, and U. Spagnolini, "Pilot-based channel estimation for OFDM systems by tracking the delay-subspace," *IEEE Trans. Wireless Commun.*, vol. 3, no. 1, pp. 315–325, Jan. 2004.
[20] D. Morris and A. H. Aghvami, "A novel location management scheme for cellular overlay networks," *IEEE Trans. Broadcast.*, vol. 52, no. 1, pp. 108–115, Mar. 2006.
[21] D. Morris and A. H. Aghvami, "Location management strategies for cellular overlay networks—A signaling cost analysis," *IEEE Trans. Broadcast.*, vol. 53, no. 2, pp. 480–493, Jun. 2007.
[22] X. Wang, Y. Wu, and J.-Y. Chouinard, "Robust data transmission using the transmitter identification sequences in ATSC DTV signals," *IEEE Trans. Consum. Electron.*, vol. 51, no. 1, pp. 41–47, Feb. 2005.
[23] S. I. Park, H. M. Kim, Y. Wu, and J. Kim, "Field test results of additional data transmission for the ATSC terrestrial DTV system," *IEEE Trans. Broadcast.*, vol. 60, no. 4, pp. 724–727, Dec. 2014.
[24] S. Jeong, O. Simeone, A. Haimovich, and J. Kang, "Beamforming design for joint localization and data transmission in distributed antenna system," *IEEE Trans. Veh. Technol.*, vol. 64, no. 1, pp. 62–76, Jan. 2015.
[25] S. Jeong, O. Simeone, and J. Kang, "Optimization of massive full-dimensional MIMO for positioning and communication," *IEEE Trans. Wireless Commun.*, vol. 17, no. 9, pp. 6205–6217, Sep. 2018.
[26] D. V. Sarwate and M. B. Pursley, "Crosscorrelation properties of pseudorandom and related sequences," *Proc. IEEE*, vol. 68, no. 5, pp. 593–619, May 1980.
[27] D. Jourdan, D. Dardari, and M. Win, "Position error bound for UWB localization in dense cluttered environments," *IEEE Trans. Aerosp. Electron. Syst.*, vol. 44, no. 2, pp. 613–628, Apr. 2008.
[28] S. Ahn, S.-I. Park, J.-Y. Lee, S. Kwon, B.-M. Lim, H. M. Kim, N. Hur, and J. Kim, "Cramer-Rao bound analysis on RF-watermark TxID detection in SFN with randomly distributed Co-channel interferers," in *Proc. IEEE Int. Symp. Broadband Multimedia Syst. Broadcast. (BMSB)*, Jeju, South Korea, Jun. 2019, pp. 1–3.
[29] H. C. So, Y. T. Chan, and F. K. W. Chan, "Closed-form formulae for Time-Difference-of-Arrival estimation," *IEEE Trans. Signal Process.*, vol. 56, no. 6, pp. 2614–2620, Jun. 2008.
[30] J. G. Andrews, F. Baccelli, and R. K. Ganti, "A tractable approach to coverage and rate in cellular networks," *IEEE Trans. Commun.*, vol. 59, no. 11, pp. 3122–3134, Nov. 2011.
[31] A. Shojaeifard, K. A. Hamdi, E. Alsusa, D. K. C. So, and J. Tang, "Exact SINR statistics in the presence of heterogeneous interferers," *IEEE Trans. Inf. Theory*, vol. 61, no. 12, pp. 6759–6773, Dec. 2015.
[32] S. Ahn, S.-I. Park, J.-Y. Lee, N. Hur, Y. Wu, L. Zhang, W. Li, and J. Kim, "Large-scale network analysis on NOMA-aided Broadcast/Unicast joint transmission scenarios considering content popularity," *IEEE Trans. Broadcast.*, early access, Jan. 27, 2020, doi: 10.1109/TBC.2020.2965062.
[33] B.-M. Lim, S. Kwon, S. Ahn, S. I. Park, J.-Y. Lee, N. Hur, H. Mook Kim, and J. Kim, "Laboratory test analysis of TxID impact into ATSC 3.0 preamble," in *Proc. IEEE Int. Symp. Broadband Multimedia Syst. Broadcast. (BMSB)*, Valencia, Spain, Jun. 2018, pp. 1–3.
[34] S. Jeon, J. Lee, S. Kwon, B.-M. Lim, S. Ahn, Y.-S. Shin, J.-Y. Lee, and S.-I. Park, "Field trial results for ATSC 3.0 TxID transmission and detection in single frequency network of Seoul," in *Proc. IEEE Int. Symp. Broadband Multimedia Syst. Broadcast. (BMSB)*, Valencia, Spain, Jun. 2018, pp. 1–4.

**SUNGJUN AHN** (Member, IEEE) received the B.S. and M.S. degrees in electrical engineering from the Korea Advanced Institute of Science and Technology (KAIST), Daejeon, South Korea, in 2015 and 2017, respectively. He has been with the Media Research Division, Electronics and Telecommunications Research Institute (ETRI), since 2017, where he is currently a Research Engineer. His research interests include stochastic geometry analysis, signal processing, and optimization for wireless communications and digital broadcasting.

**SUNG-IK PARK** (Senior Member, IEEE) received the B.S.E.E. degree from Hanyang University, Seoul, South Korea, in 2000, the M.S.E.E. degree from POSTECH, Pohang, South Korea, in 2002, and the Ph.D. degree from Chungnam National University, Daejeon, South Korea, in 2011. Since 2002, he has been with the Broadcasting System Research Group, Electronics and Telecommunication Research Institute (ETRI), where he is currently a Project Leader and a Principal Member of research staff. His research interests are in the area of error correction codes and digital communications, in particular, signal processing for digital television. He has over 200 peer-reviewed journal and conference publications, and multiple best paper and contribution awards for his work on broadcasting technologies. He serves as an Associate Editor for the IEEE TRANSACTIONS ON BROADCASTING and *ETRI Journal*, and a Distinguished Lecturer of IEEE Broadcasting Technology Society.

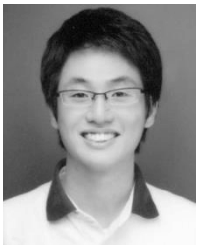

**SUNHYOUNG KWON** (Member, IEEE) received the B.S. degree in electrical communications engineering from Information and Communications University, Daejeon, South Korea, in 2008, and the M.S. and Ph.D. degrees in electrical engineering from the Korea Advanced Institute of Science and Technology, Daejeon, in 2010 and 2020, respectively. Since 2010, he has been with the Broadcasting System Research Group, Electronics and Telecommunication Research Institute, where he is currently a Senior Member of research staff. His research interests are in the area of digital broadcasting and communications.

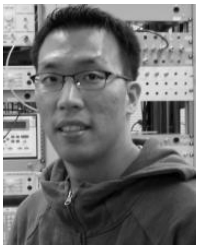

**JAE-YOUNG LEE** (Senior Member, IEEE) received the B.S. degree (Hons.) in electrical and computer engineering from Rutgers University, in 2001, the M.S. degree in electrical and computer engineering from the University of Wisconsin at Madison, in 2003, and the Ph.D. degree in engineering science from Simon Fraser University, in 2013. He joined the Electronics and Telecommunications Research Institute (ETRI), in 2003. He is currently a Principal Research Associate with the Broadcasting Systems Research Group, ETRI. His research interests are in the areas of digital signal processing for various applications, including digital broadcasting, telecommunications, and human–computer interaction systems.

**NAMHO HUR** (Member, IEEE) received the B.S., M.S., and Ph.D. degrees in electrical and electronic engineering from the Pohang University of Science and Technology, Pohang, South Korea, in 1992, 1994, and 2000, respectively. He is currently with the Telecommunications and Media Research Laboratory, Electronics and Telecommunications Research Institute, Daejeon, South Korea, where he is also the Project Leader of Development of Transmission Technology for Ultra High Quality UHD. His research interest includes realistic digital broadcasting systems. He was the Chair of Future of Broadcast Television Initiative (FOBTV) Management Committee, from April 2018 to April 2019.